Generation of heralded optical cat states by photon addition

Yi-Ru Chen,[1] Hsien-Yi Hsieh,[1] Jingyu Ning,[1] Hsun-Chung Wu,[1] Hua Li Chen,[2] Zi-Hao Shi,[1] Popo Yang,[1] Ole Steuernagel,[1] Chien-Ming Wu,[1] and Ray-Kuang Lee[1,2,3,4,*]

[1]*Institute of Photonics Technologies, National Tsing Hua University, Hsinchu 30013, Taiwan*
[2]*Department of Physics, National Tsing Hua University, Hsinchu 30013, Taiwan*
[3]*Center for Theory and Computation, National Tsing Hua University, Hsinchu 30013, Taiwan*
[4]*Center for Quantum Science and Technology, Hsinchu 30013, Taiwan*

(Received 20 October 2023; revised 24 June 2024; accepted 12 July 2024; published 1 August 2024)

Optical cat states, the nonclassical superposition of two quasi-classical coherent states, serve as a basis for gedankenexperiments testing quantum physics on mesoscopic scales and are increasingly recognized as a resource for quantum information processing. Here, we report the first experimental realization of optical cat states by adding a photon to a squeezed vacuum state; so far only photon-subtraction protocols have been realized. Photon addition gives us the advantage of using heralded signal photons as experimental triggers, and we can generate cat states at rates exceeding 2.3×10^5 counts per second. Our most highly squeezed vacuum input state shows -8.9 dB squeezing, but such squeezing entails some degradation—in this case, 15.1 dB antisqueezing. Even so, our approach enables us to synthesize a state with a maximum cat amplitude of $|\alpha| \approx 1.77$ whose Wigner distribution still shows pronounced negative parts. Our experimental implementation with controlled photon addition demonstrates a powerful and robust building block for advanced quantum state engineering and shows that heralded photon addition can be controlled well and performed at high rates.

DOI: 10.1103/PhysRevA.110.023703

I. INTRODUCTION

Coherent laser fields described by the quantum state $|\alpha\rangle$ can be put into a mesoscopic superposition of two such states $|\alpha\rangle - |-\alpha\rangle$ [1–3]. Here, the light field is superposed in such a way that the relative phase between the individual components leads to destructive interference at the center. Such superposition states are called optical Schrödinger "cat states," in honor of Erwin Schrödinger's famous *gedankenexperiments* to illustrate paradoxa of quantum physics [4].

Optical cat states are important as tools for testing macroscopic limits of quantum physics and also for many quantum computation and communication protocols [5,6]. But, they are hard to generate and so far only available at low production rate and low amplitudes, when using photon-subtraction schemes [7].

Using an optical parametric oscillator (OPO), photon subtraction from a squeezed vacuum state has been implemented for the generation of optical cat states [8,9]. Production of cat states based on controlled removal of a single photon has to use either weakly reflecting mirrors, via beam splitters, or perfectly photon number resolving detectors, to avoid damage to the desired output states. This *passive* approach with beam splitters, while simpler in implementation, badly limits the success rate of such subtraction approaches.

To boost the state's usefulness for fundamental and practical applications, more complicated schemes have been attempted to enlarge the size of optical cat states, such as using two-photon Fock states [10], ancilla-assisted photon subtraction [11], optical synthesis [12], in-line amplification through optical parametric amplifiers [13], subtraction from multimodes [14], and generalized photon subtraction with two-mode squeezers [15]. Even though high purity and entanglement of optical cat states [16,17], as well as remote preparation of nonlocal superpositions [18], have been demonstrated, a high generation rate is crucial for practical applications of such superpositions in fundamental tests and quantum information protocols.

To go beyond these constrains, here, we report the first experimental realization of photon addition for the generation of quantum-optical "negative cat" mesoscopic superposition states, of the form

$$\Psi_- = N_\alpha(|\alpha\rangle - |-\alpha\rangle), \tag{1}$$

from highly squeezed input states. Here, N_α is the normalization constant.

Using photon addition as an *active* approach has three immediate advantages over the traditional photon-subtraction approach: the generation rate increases by at least one order of magnitude, the states are nonclassical even for high initial squeezing and low initial state purity, and the amplitude $|\alpha|$ of the final state very desirably increases when using repeated photon addition, instead of decreasing it, as is unavoidable when using repeated photon subtraction. We note that the addition of a single photon to a pure squeezed vacuum state gives exactly the same outcome as the subtraction of a single photon [19], yet significant benefits in photon addition

*Contact author: rklee@ee.nthu.edu.tw

arise for experiments using impure squeezed vacuum [20], as shown in Fig. 3.

The earliest theoretical proposal for photon addition to coherent states [21] was soon followed by those for addition to a squeezed vacuum state [22,23]. Even though the demonstration of photon addition to coherent states of light [24], as well as the test of quantum commutation rules for thermal states, was reported experimentally [25,26], the realization of photon addition to squeezed states has been missing for two decades. Here, we fill this experimental gap by adding a single photon to a squeezed vacuum state; both constituent states have no classical counterpart.

Contrasted with photon subtraction, photon addition from an entangled photon pair is generated in *stimulated* parametric down conversion (StPDC). This allows us to use one of the pair as a heralding photon to monitor success whilst the other one is added to a squeezed vacuum state, as the input seed also substantially increasing production rates. Therefore, only through photon addition can we reasonably hope to add more photons in further stages whilst preserving, or even enhancing further, the nonclassical nature of the final state.

A pure squeezed vacuum state $|\xi\rangle$, to which m photons are added, has the form $|\xi, m\rangle = \frac{1}{\sqrt{N_m(|\xi|)}}(\hat{a}^\dagger)^m|\xi\rangle$. Here, $N_m(|\xi|) = m!(1-|\xi|^2)^{-m/2}P_m[(1-|\xi|^2)^{-1/2}]$ is the normalization factor with Legendre polynomials P_m [23].

In the case of one added photon ($m = 1$), the single-photon-added pure squeezed vacuum state is $|\xi, 1\rangle = \frac{\hat{a}^\dagger|\xi\rangle}{\sqrt{N_1(|\xi|)}}$ and only a negative-cat superposition state Ψ_- (1) can result [27,28]. This is achieved using the signal photon of photon pairs from StPDC, formally

$$|\psi\rangle \approx (1 + g\hat{a}_s^\dagger\hat{a}_i^\dagger)|\xi\rangle_s|0\rangle_i = |\xi\rangle_s|0\rangle_i + g\hat{a}_s^\dagger|\xi\rangle_s|1\rangle_i. \quad (2)$$

Here, g is the gain factor of the StPDC process, and $\hat{a}_s^\dagger$ and $\hat{a}_i^\dagger$ are signal and idler photon creation operators, respectively. Compared to the probabilistic process in spontaneous parametric down conversion (SPDC), the StPDC gain provides a control in applying photon addition.

The remainder of this paper is organized as follows. In Sec. II details about our experimental implementation are illustrated. Then, in Sec. III we demonstrate the experimental results on the generation of optical cat states by photon adding, with input squeezed states for high- and low-purity conditions. In Sec. IV, we discuss the advantage in applying photon addition. Finally, we conclude our results in Sec. V.

II. EXPERIMENTS

As sketched in Fig. 1(a), we initially generate squeezed vacuum states in a bow-tie OPO cavity enclosing a periodically poled nonlinear $KTiOPO_4$ (PPKTP) crystal with second-order nonlinear susceptibility $\chi^{(2)}$, operated below the lasing threshold, at wavelength 1064 nm [29]. This OPO cavity has an optical path length of approximately 285 mm, with a finesse of 19.8 at 532 nm and of 33.4 at 1064 nm. The overall efficiency, $1-L$ (where L is the loss), is 89.45% $\pm$ 1.12% and the phase noise is 18.44 ± 4.55 mrad.

Then, the OPO-generated squeezed vacuum states $\varrho_{\rm sq}^{\rm OPO}$ are subsequently injected into a type-II StPDC crystal which is inside another bow-tie cavity of the same configuration as

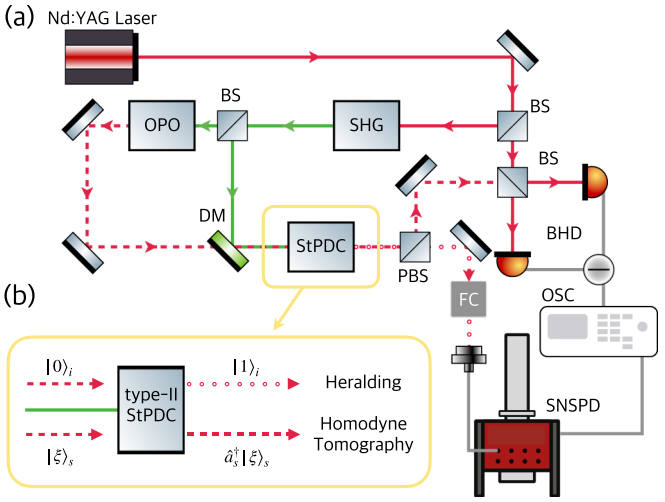

FIG. 1. Schematic diagram of the experimental setup. (a) The squeezed vacuum beam $|\xi\rangle_s$ is produced by the OPO and injected into the type-II StPDC to perform the photon-addition scheme $\hat{a}_s^\dagger|\xi\rangle_s$. (b) After passing through the filter cavity (FC), the idler single-photon state $|1\rangle_i$ is used as the heralding signal, collected by the superconducting nanowire single-photon detector (SNSPD). The optical cat state, i.e., photon-added squeezed state, is characterized by homodyne tomography with BHD. The setup also includes a beam splitter (BS), dichroic mirrors (DM), a polarization beam splitter (PBS), a second-harmonic generator (SHG), and an oscilloscope (OSC).

the OPO cavity, i.e., also 285 mm in length, with FWHM of 31.8 MHz. It performs the photon addition [symbolically $\hat{a}_s^\dagger|\xi\rangle_s$ in Fig. 1(b)].

To ensure a coherent addition process, the filtering plays a critical role in our experiments since it ensures that, at a time, only a single photon is added into the squeezed vacuum.

The OPO cavity's free spectral range is 1.052 GHz, giving rise to neighboring modes, which we suppress with filter cavities, consisting of one triangle cavity followed by two Fabry-Perot cavities, with FWHM of 16.3, 131, and 101 MHz, respectively. The filter cavity system has a narrow band compared with StPDC and OPO cavities in order to purify the cat state (see Appendix A).

The StPDC pair's idler photon gets detected by a superconducting nanowire single-photon detector, generating the heralding trigger signal for the balanced homodyne detector (BHD). Our homodyne detector's bandwidth is 7.45 MHz and the detection efficiency is estimated at 92%, which is composed of the quantum efficiency of photodiodes (99%), homodyne visibility efficiency (96%), and the circuit noise of homodyne detection (97%). The BHD output is then integrated after convolution with a double-decayed (two time constants) temporal mode function, see Appendixes C and D.

In the absence of squeezed light ($P_{\rm OPO} = 0$), using the pairs' idler photons as triggers, we perform quantum state tomography for Fock number states in this SPDC process, in order to characterize the output single photon. By optimizing the negativity from the output single-photon Wigner distribution with a variable pump power, pumping at 10 mW, our StPDC cavity gives a minimum value of $W(0,0) = -0.0643$,

TABLE I. Results summary for a fixed SPDC pump power of 10 mW at different OPO pump-power levels P_{OPO} (OPO threshold power of $P_{\mathrm{th}} = 103.9$ mW, hence power relative to threshold $P_{\mathrm{rel}} = P_{\mathrm{OPO}}/P_{\mathrm{th}}$ in percentage), column 1. Columns 2 and 3, SQ and ASQ levels for state $\varrho_{\mathrm{sq}}^{\mathrm{OPO}}$ right after the OPO and its purity. Column 4, SQ:ASQ values obtained after the empty SPDC cavity (without pump field, i.e., for $\varrho_{\mathrm{sq}}^{\mathrm{empty}}$). Column 5, purity of the output state $\varrho_{\mathrm{sq}}^{\mathrm{add}}$ after performing the photon addition and, column 6, its negative Wigner distribution values $W[\varrho_{\mathrm{sq}}^{\mathrm{add}}](0,0)$. Fidelities with respect to Glauber cat states (1) and photon-added impure squeezed states (3), columns 7 and 8. Cat size $|\alpha|$ and generation rates Γ, columns 9 and 10. All squeezing data are measured within 1 MHz.

P_{OPO} (P_{rel}%)	SQ:ASQ ($\varrho_{\mathrm{sq}}^{\mathrm{OPO}}$)	Purity ($\varrho_{\mathrm{sq}}^{\mathrm{OPO}}$)	SQ:ASQ ($\varrho_{\mathrm{sq}}^{\mathrm{empty}}$)	Purity ($\varrho_{\mathrm{sq}}^{\mathrm{add}}$)	$W[\varrho_{\mathrm{sq}}^{\mathrm{add}}](0,0)$	F_{cat}	$F_{\mathrm{sq}}^{\mathrm{add}}$	Cat size ($\lvert\alpha\rvert$)	Γ (counts/s)
5 mW (5%)	−3.8:3.9 dB	0.99	−0.3:0.3 dB	0.55	−0.094	64%	64%	0.40	6.0×10^4
20 mW (19%)	−6.3:7.3 dB	0.89	−1.2:1.7 dB	0.52	−0.092	64%	63%	0.74	6.1×10^4
40 mW (38%)	−7.6:11.6 dB	0.63	−3.2:4.3 dB	0.43	−0.052	55%	72%	1.24	8.1×10^4
60 mW (58%)	−8.9:15.1 dB	0.49	−3.2:9.9 dB	0.33	−0.008	39%	80%	1.77	23.5×10^4

with a purity of 0.53 for the signal photons, along with their second-order correlation function value of $g^{(2)}(0) \approx 0.55$ [30]. At the same time, we measure a photon-pair generation rate of $\Gamma = 6.0 \times 10^4$ Hz, with 60.1% and 37.6% in the output single-photon and vacuum states, see Appendix B.

This StPDC pump power of 10 mW is therefore from now on chosen and kept fixed while we generate photon-added squeezed states at different OPO pump powers, and hence different levels of squeezing ξ, namely, at 5, 20, 40, and 60 mW, see Table I.

III. PHOTON-ADDED SQUEEZED STATES

Due to unavoidable coupling to the environment, in our experiment, the squeezed vacuum state $\varrho_{\mathrm{sq}}^{\mathrm{OPO}}$ at the output of the OPO is degraded. The magnitudes of squeezing (SQ) versus antisqueezing (ASQ), at the output of the OPO, $\varrho_{\mathrm{sq}}^{\mathrm{OPO}}$, are almost the same at a low pump power of 5 mW, specifically, SQ:ASQ = −3.8:3.9 dB [31]. At the highest pump power of 60 mW, the squeezing ratio is SQ:ASQ = −8.9:15.1 dB. Simultaneously, the purity of the squeezed vacuum drops from 0.99 to 0.49, see columns 2 and 3 of Table I below.

To evaluate the optical losses when applying a StPDC cavity to perform photon addition, the SQ:ASQ levels are additionally measured after the StPDC cavity, without applying StPDC pump power, yielding the quantum state $\varrho_{\mathrm{sq}}^{\mathrm{empty}} = \mathcal{L}[\varrho_{\mathrm{sq}}^{\mathrm{OPO}}]$, where $\mathcal{L}$ is a Lindbladian superoperator describing the effects of the empty StPDC cavity, see column 4 of Table I. We do not model these effects explicitly but determine the losses due to the presence of the empty StPDC cavity in the experimental reconstruction of $\varrho_{\mathrm{sq}}^{\mathrm{empty}}$, which subsequently serves as our benchmark for the quantification of the relative fidelity $F_{\mathrm{sq}}^{\mathrm{add}}$ of the photon-addition process.

In the following, we apply two figures of merit to characterize the performance in the generation of optical cat states by photon addition, i.e., the cat fidelity F_{cat} and the relative fidelity $F_{\mathrm{sq}}^{\mathrm{add}}$.

By comparing our experimentally reconstructed state $\varrho_{\mathrm{sq}}^{\mathrm{add}}$ with the ideal Glauber cat state $(|\alpha\rangle - |-\alpha\rangle)$, we calculate its cat fidelity F_{cat}. This fidelity remains higher than 55% even when working at the OPO pump power of 40 mW, but at 60 mW pump power it drops to 39%, see Table I column 7. We will now explain that this drop in fidelity is a poor measure of the good performance of photon addition. Instead, photon addition is better quantified by the relative fidelity $F_{\mathrm{sq}}^{\mathrm{add}}$ with respect to state (3), see Table I column 8.

When we introduced the negative cat state Ψ_- of Eq. (1), based on Glauber states, we emphasized that our squeezing levels, at the current limit of technology for the generation of squeezed states, are so high that descriptions by Glauber states as constituents become ill-matched because Glauber states have the width of unsqueezed vacuum states. Because of this mismatch, instead of developing a complicated theoretical model, we determine the performance of our photon-addition setup by itself. We do this in the following way:

We experimentally determine the injected squeezed state $\varrho_{\mathrm{sq}}^{\mathrm{empty}}$ [31] and its degradation.

We then theoretically determine its form after applying ideal photon addition to it,

$$\hat{\rho}_{\mathrm{sq}}^{\mathrm{add}} = N_{\mathrm{add}}\, \hat{a}_s^\dagger\, \varrho_{\mathrm{sq}}^{\mathrm{empty}}\, \hat{a}_s, \tag{3}$$

where N_{add} is the normalization constant.

Note that we use the denotations "$\hat{\rho}$" for theoretical and "ϱ" for experimentally reconstructed quantum states.

The *experimentally reconstructed* density matrix $\varrho_{\mathrm{sq}}^{\mathrm{add}}$ is then compared to $\hat{\rho}_{\mathrm{sq}}^{\mathrm{add}}$, allowing us to extract the fidelity due to the photon-addition process by itself, see Table I column 8.

For the addition of a single photon by itself, determined with respect to the degraded input state $\varrho_{\mathrm{sq}}^{\mathrm{empty}}$, in Eq. (3), we reach the associated relative fidelity $F_{\mathrm{sq}}^{\mathrm{add}}$ of 80% (or a fidelity of 39% for an optical cat with a maximum cat size $|\alpha| \approx 1.77$). This happens at a generation rate of 2.35×10^5 counts per second, at least one order of magnitude higher than all previously reported rates (which are all based on photon subtraction).

Tomographic reconstructions of the Wigner distributions $W[\varrho_{\mathrm{sq}}^{\mathrm{add}}]$ (from BHD data, see Fig. 1) are shown in Figs. 2(e)–2(h).

A. Input squeezed states with high purity

In Figs. 2(a) and 2(e), we display the Wigner distribution when using low OPO pump power of $P_{\mathrm{OPO}} = 5$ mW. The experimentally reconstructed state $\varrho_{\mathrm{sq}}^{\mathrm{add}}$ has a purity of 0.55 and a negative value of $W[\varrho_{\mathrm{sq}}^{\mathrm{add}}](0,0) = -0.094$. Comparison between experimental Wigner distributions and Glauber-cat reference states Ψ_- of Eq. (1) give good agreement at such low pump-power levels, as the degradation in the injected squeezed vacuum states is not severe. Maximizing the fidelity

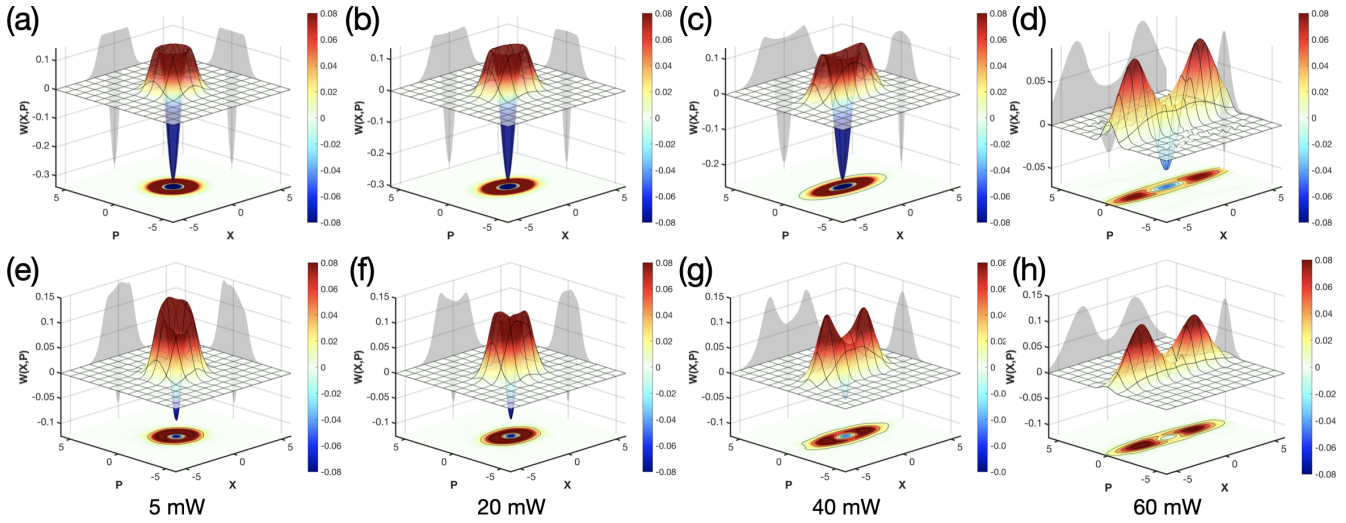

FIG. 2. Wigner distributions of optical cat states: (a–d) for the theoretical photon-added squeezed states, $W[\hat{\rho}_{\rm sq}^{\rm add}]$ of Eq. (3); and (e–h) for experimental data with 92% detection efficiency correction, $W[\varrho_{\rm sq}^{\rm add}]$, obtained with OPO pump powers at $P_{\rm OPO} = 5$, 20, 40, and 60 mW, respectively.

with respect to an ideal Glauber cat state Ψ_- allows us to estimate the amplitude of our cat state as $|\alpha| = 0.40$, see Table I column 9.

Overall, we observe a maximum negativity of -0.094 at an OPO pump power of 5 mW when the purity of our generated optical cat states also reaches its largest value.

B. Impure input squeezed states with low purity

When we increase the OPO pump power to 20 and 40 mW, the OPO output state $\varrho_{\rm sq}^{\rm OPO}$ starts to show degraded squeezing levels, SQ:ASQ $= -6.3$:7.3 dB and -7.6:11.6 dB, see Table I column 2. Yet, despite this degradation, the purity in the target cat states remains as high as that from the nearly perfectly pure squeezed state, i.e., 0.52 and 0.43, respectively, see Table I column 5. For both cases, the negativity remains pronounced and the amplitude of our cat states enlarges to $|\alpha| = 0.74$ and 1.24, respectively. See Table I columns 6 and 9, and Figs. 2(f) and 2(g) for the associated Wigner distributions $W[\varrho_{\rm sq}^{\rm add}]$.

Finally, we reach an OPO pump power of 60 mW. Now, the OPO output state $\varrho_{\rm sq}^{\rm OPO}$ shows further degraded squeezing levels and a low purity of 0.49, see Table I column 3. Therefore, the final optical cat state $\varrho_{\rm sq}^{\rm add}$ also has a low purity of 0.33, see Table I column 5. The associated cat amplitude is large, $|\alpha| = 1.77$, see Table I column 9 and Fig. 2(h).

Most surprisingly, however, despite the input state $\varrho_{\rm sq}^{\rm OPO}$'s low purity (at 60 mW OPO pump power) and a noisy environment, using photon addition lets the optical cat survive: it shows a clear negative value of $W[\varrho_{\rm sq}^{\rm add}](0, 0) = -0.008$. As a comparison, theoretically, we have a negative value of $W[\hat{\rho}_{\rm sq}^{\rm add}](0, 0) = -0.059$, as shown in Fig. 2(d).

IV. DISCUSSION

It is known that, when applying photon subtraction, the input squeezed states must be pure enough, practically limiting the input state's squeezing to no less than -5 dB. Additionally, repeated application of photon subtraction drives states toward the vacuum state [32]. By contrast, our photon-addition scheme can support the generation of optical cat states with higher squeezing levels, even as the input squeezed states become increasingly impure.

We reach initial squeezing levels as low as -8.9 dB, with a purity of 0.49 (or squeezing levels at -3.2 dB with a purity of 0.33 after the StPDC cavity), see Fig. 1. Photon addition is so tolerant to experimental imperfections that we still observe pronounced negative parts in the Wigner distribution all the way down to -8.9 dB in squeezing, even though the input squeezed state has low purity, see Table I column 6.

Even though the addition of a single photon to a pure squeezed state gives exactly the same outcome as the subtraction of a single photon, this equivalence of outcome no longer holds when the input state is impure [19]. To illustrate the advantage of photon addition, we consider the experimental data by modeling degraded squeezed states as

$$\hat{\rho}^{\rm deg} \equiv (1 - c)\hat{\rho}^{\rm pure} + c\,\hat{\rho}^{\rm thermal}, \tag{4}$$

with $\hat{\rho}^{\rm pure} = |\xi\rangle\langle\xi|$ from the experimentally measured squeezing levels and $\hat{\rho}^{\rm thermal}$ with a thermal average photon number $n_{\rm th} = [0, 0.5]$, used for fitting, see Ref. [31]. We vary the probability parameter $c : [0, 1]$ to simulate the purity of the input squeezed states, i.e., $\mathrm{tr}[(\hat{\rho}^{\rm deg})^2]$.

For photon addition or photon subtraction applied to the degraded squeezed states given in Eq. (4), the output states are calculated by $\hat{\rho}^{\rm add} = \hat{a}_s^\dagger\,\hat{\rho}^{\rm deg}\,\hat{a}_s$ and $\hat{\rho}^{\rm sub} = \hat{a}_s\,\hat{\rho}^{\rm deg}\,\hat{a}_s^\dagger$, respectively. Then, in Fig. 3, we plot the theoretical curve for the fidelity of optical cat generation by fixing the cat size $|\alpha| = 1.02$, as a function of the purity of the squeezed input states.

Figure 3 demonstrates the advantage in applying photon addition over photon subtraction. In particular, when the purity of input squeezed states decreases, the benefits from

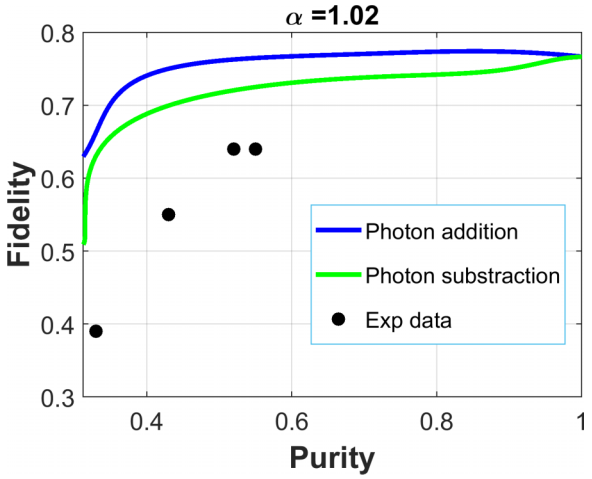

FIG. 3. Theoretically determined fidelities of the generation of Glauber cat states as a function of the input squeezed states' purity (contrasting photon addition, blue curve, with subtraction, green curve) predict greater robustness for photon addition processes. Four experimentally generated data points, $\varrho_{\rm sq}^{\rm add}$ in Table I column 5, are given for OPO pump power at 5, 20, 40, and 60 mW, respectively, roughly confirming the plot trends.

photon addition become more significant. Without considering the cavity losses, our experimental data, also shown in Fig. 3, confirm the trends with the imperfections in implementations.

This analysis confirms that photon addition is robust. Adding a photon to a highly squeezed impure input state has a high relative fidelity $F_{\rm sq}^{\rm add}$ value ranging from 64% at 5 mW to 80% at 60 mW, see Table I column 8. This shows that photon addition can be fairly well controlled, even at high generation rates.

V. CONCLUSIONS

We have shown that photon addition can be applied to a highly squeezed input state with a squeezing level SQ of −8.9 dB. This corresponds to a cat state with an amplitude of 1.77 and a fidelity for the photon-addition process of 80% whilst maintaining control through the use of idler photons at a generation rate of 23.5 $\times 10^4$ per second; this is at least one order of magnitude higher than all previously reported rates. The observed increase in pair-generation rates Γ with increasing OPO-pump power, see Table I, is due to induced emission into the more highly excited squeezed input mode.

Our experiments thus overturn the common belief that sequential application of photon addition through multiple OPOs would involve significant losses and is therefore not advisable in experimental practice [33]. As shown in Table I, the mode matching and losses from the StPDC cavity indeed undermine the prepared SQ levels. However, as higher SQ levels are routinely generated nowadays, our successful generation of heralded optical cat states by photon addition opens up the possibility of the generation of new types of nonclassical states by repeatedly adding photons [34].

We emphasize that imperfections of our experiment are to a considerable extent due to the fact that the squeezed states we start from have reduced levels of purity when they are highly squeezed. In other words, the synthesis of highly squeezed states with high purity remains a desirable and partially unfulfilled goal of the quantum optics community. By contrast, we establish here that the addition of a photon can already be controlled to a surprisingly good degree, in particular for the impure squeezed states in practical scenarios.

Controlled photon addition promises to become a new powerful building block for advanced quantum state synthesis. With such a high generation rate, our photon-addition approach also promises to facilitate applications in quantum information processing using cat codes [35,36] or preparing error-correcting codes [37–41].

ACKNOWLEDGMENTS

This work is partially supported by the National Science and Technology Council, Taiwan (Grants No. 112-2123-M-007-001, No. 112-2119-M-008-007, and No. 112-2119-M-007-006); the Office of Naval Research Global; the International Technology Center Indo-Pacific (ITC IPAC) and Army Research Office, under Contract No. FA5209-21-P-0158, and the collaborative research program of the Institute for Cosmic Ray Research (ICRR) at the University of Tokyo.

APPENDIX A: CAVITIES TO PERFORM PHOTON ADDITION

Details about the cavities used in our experiments are given in Table II.

TABLE II. SPDC: spontaneous parametric down conversion; FC: filter cavity; FSR: free spectral range; FWHM: full width at half maximum; and HR: high reflectivity.

Cavity	Shape	Length (mm)	Reflectivities	FSR (GHz)	FWHM (MHz)
SPDC	Bow tie	285	0.83, 0.999, 0.999, 0.9985	1.052	31.8
FC1	Triangle	300	0.95, HR, 0.95	0.999	16.3
FC2	Fabry-Perot	2.2	0.994, 0.994	68.1	131
FC3	Fabry-Perot	2.85	0.994, 0.994	52.6	101

TABLE III. The fitting parameters used for the degradation due to the empty StPDC cavity.

P_{OPO} (P_{rel}%)	SQ:ASQ ($\varrho_{\mathrm{sq}}^{\mathrm{empty}}$)	Fitting parameter r	Fitting parameter n_{th}
5 mW (5%)	−0.3:0.3 dB	0.3	0.0000
20 mW (19%)	−1.2:1.7 dB	1.455	0.0296
40 mW (38%)	−3.2:4.3 dB	3.759	0.0662
60 mW (58%)	−3.2:9.9 dB	6.565	0.5800

APPENDIX B: SINGLE-PHOTON STATES

Without the OPO pump power, i.e., $P_{\mathrm{OPO}} = 0$, quantum state tomography is also applied to our single-photon state, which gives a purity of 0.53 with a negativity in $W(0,0) = -0.085$. At the same time, the generation rate at the output is 6.0×10^4 counts per second.

With the machine-learning Fock state tomography, in Fig. 4 with SPDC pump power at 10 mW, we plot the measured probability density in the quadrature from homodyne tomography data, the corresponding Wigner distribution function in the phase space, and the reconstructed photon number probability distribution. Here, we have 60.1% in the single-photon state, but with 37.6% and 2.3% in the vacuum and two-photon Fock states, respectively.

APPENDIX C: QUADRATURE DATA

In Figs. 5 and 6, the recorded quadrature raw data are demonstrated for our photon-added squeezed states at OPO pump power of 20 and 60 mW with a fixed 10-mW SPDC power. At the same time, the corresponding photon number distributions are also illustrated, which are the diagonal terms in the reconstructed density matrix.

APPENDIX D: BHD TEMPORAL CORRELATION FUNCTION

In Fig. 7, the temporal modes of detection in our experiments are shown for the vacuum and single-photon states (in the left panel), while the filter function applied to extract the single-photon trigger is shown in the right panel.

APPENDIX E: PARAMETERS USED FOR FITTING IN FIG. 2 OF THE MAIN TEXT

The degraded squeezed output $\varrho_{\mathrm{sq}}^{\mathrm{empty}}$, characterized by the SQ:ASQ levels, measured after the StPDC cavity, without applying StPDC pump power, is fitted by squeezed thermal states, i.e.,

$$\varrho_{\mathrm{sq}}^{\mathrm{empty}} = \hat{S}(r,\theta)\hat{\rho}_{\mathrm{th}}(n_{\mathrm{th}})\hat{S}^{\dagger}(r,\theta), \tag{A1}$$

with r, θ, and n_{th} corresponding to the squeezing ratio, squeezing angle, and the average photon number, respectively. Here, $\hat{S}(r,\theta) = \exp[\frac{1}{2}(\xi^* \hat{a}^2 - \xi \hat{a}^{\dagger 2})]$ denotes the squeezing transformation, with $\xi \equiv r\exp(i\theta)$; $r \in [0,\infty]$ and $\theta \in [0, 2\pi]$. Moreover, the thermal states are characterized with the average photon number n_{th}, reflecting the corresponding temperature in the thermal reservoir, i.e., $\bar{n}^{-1} = \exp[\hbar\omega/k_B T] - 1$. In Table III, we list the fitting parameters (r and n_{th}) used in Fig. 2 of the main text.

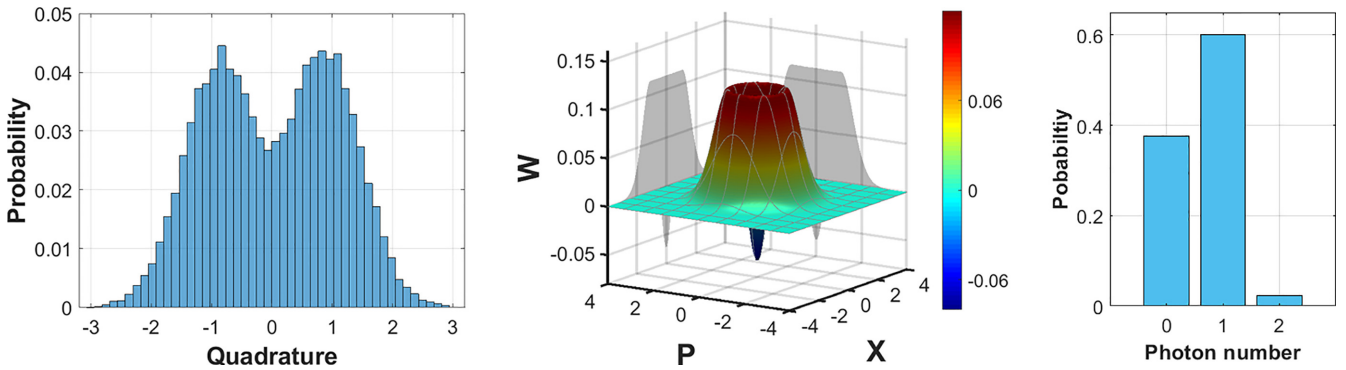

FIG. 4. (Left) The measured probability density in the quadrature from homodyne tomography data, with SPDC pump power at 10 mW. (Middle) The corresponding Wigner distribution function in phase space. (Right) The reconstructed photon number probability distribution with $p_0 = 0.376$, $p_1 = 0.601$, and $p_2 = 0.023$, corresponding to vacuum, single-photon, and two-photon Fock states, respectively.

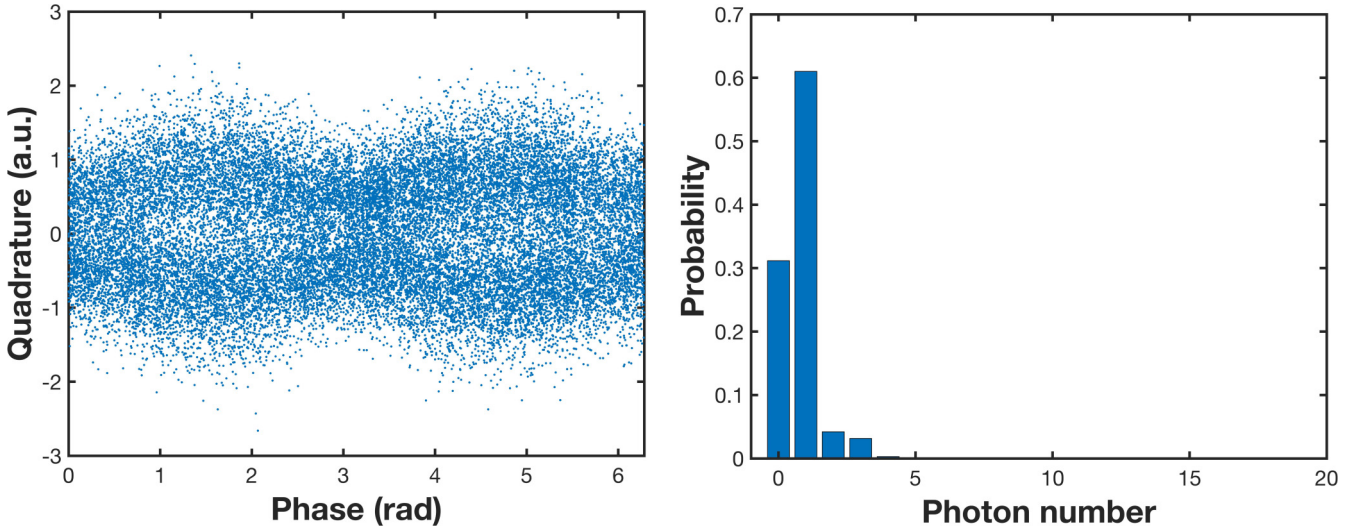

FIG. 5. Part of the recorded quadrature points at OPO pump power of 20 mW with a fixed 10-mW SPDC power, and the corresponding photon number distribution in the diagonal term of the reconstructed density matrix.

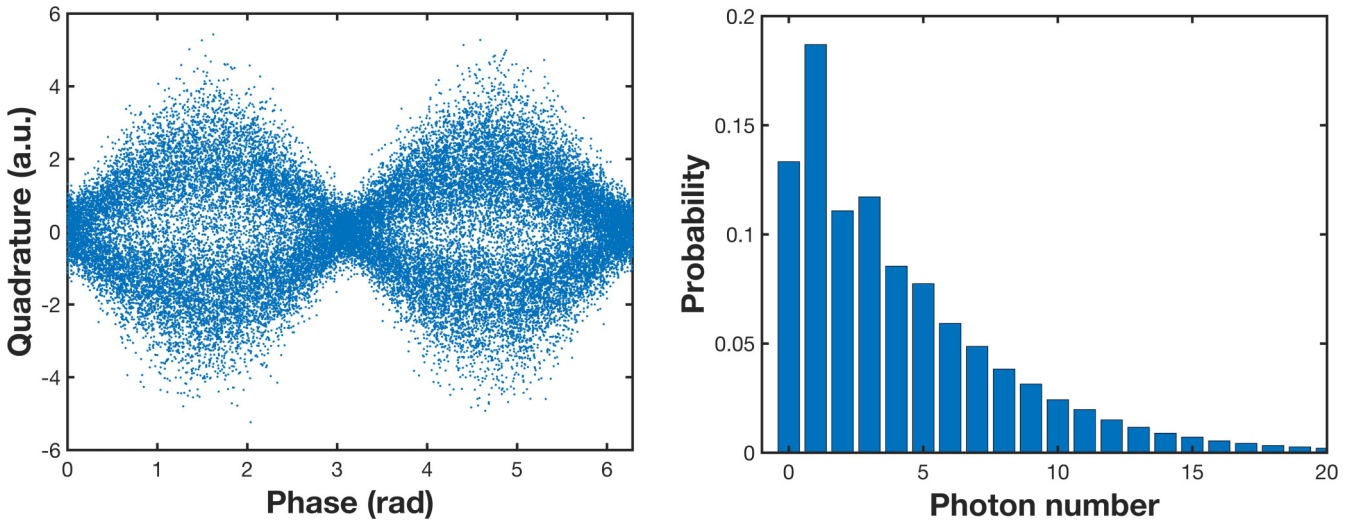

FIG. 6. Part of the recorded quadrature points at OPO pump power of 60 mW with a fixed 10-mW SPDC power, and the corresponding photon number distribution in the diagonal term of the reconstructed density matrix.

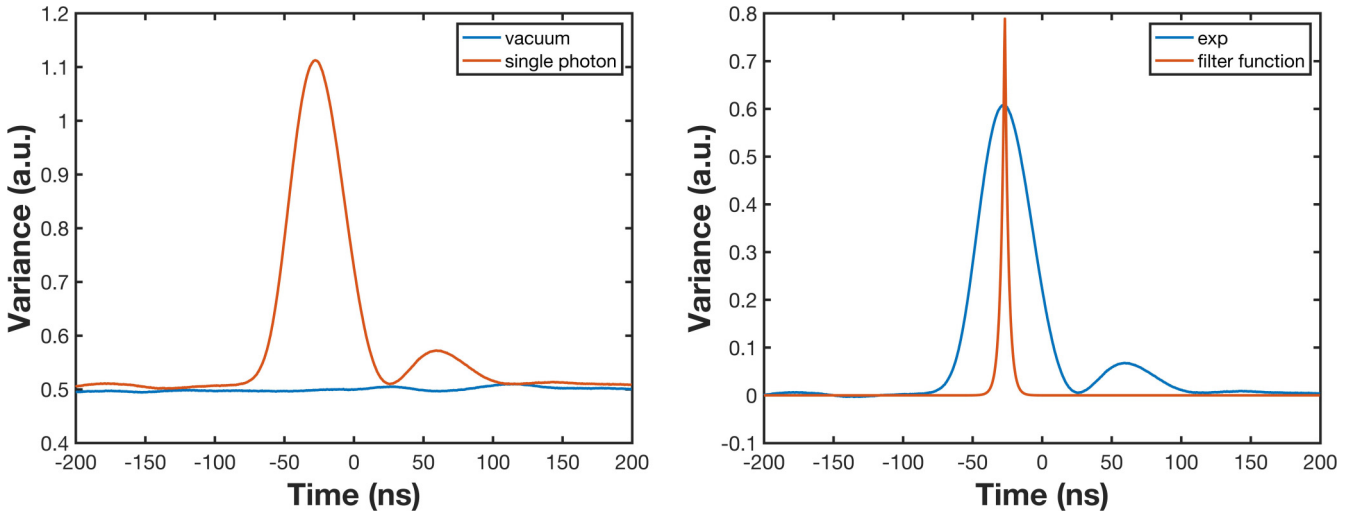

FIG. 7. (Left) Temporal correlation functions from vacuum and single photon states. (Right) The corresponding filter function used in BHD.

[1] P. Marek, H. Jeong, and M. S. Kim, Phys. Rev. A **78**, 063811 (2008).

[2] C. Navarrete-Benlloch, R. Garcia-Patron, J. H. Shapiro, and N. J. Cerf, Phys. Rev. A **86**, 012328 (2012).

[3] U. Chabaud, T. Douce, D. Markham, P. V. Loock, E. Kashefi, and G. Ferrini, Phys. Rev. A **96**, 062307 (2017).

[4] E. Schrödinger, Naturwissenschaften **23**, 807 (1935).

[5] S. L. Braunstein and P. V. Loock, Rev. Mod. Phys. **77**, 513 (2005).

[6] C. Weedbrook, S. Pirandola, R. García-Patrón, N. J. Cerf, T. C. Ralph, J. H. Shapiro, and S. Lloyd, Rev. Mod. Phys. **84**, 621 (2012).

[7] A. Ourjoumtsev, R. Tualle-Brouri, J. Laurat, and P. Grangier, Science **312**, 83 (2006).

[8] J. S. Neergaard-Nielsen, B. M. Nielsen, C. Hettich, K. Mølmer, and E. S. Polzik, Phys. Rev. Lett. **97**, 083604 (2006).

[9] K. Wakui, H. Takahashi, A. Furusawa, and M. Sasaki, Opt. Express **15**, 3568 (2007).

[10] A. Ourjoumtsev, H. Jeong, R. Tualle-Brouri, and P. Grangier, Nature (London) **448**, 784 (2007).

[11] H. Takahashi, K. Wakui, S. Suzuki, M. Takeoka, K. Hayasaka, A. Furusawa, and M. Sasaki, Phys. Rev. Lett. **101**, 233605 (2008).

[12] K. Huang, H. Le Jeannic, J. Ruaudel, V. B. Verma, M. D. Shaw, F. Marsili, S. W. Nam, E. Wu, H. Zeng, Y.-C. Jeong, R. Filip, O. Morin, and J. Laurat, Phys. Rev. Lett. **115**, 023602 (2015).

[13] M. Wang, M. Zhang, Z. Qin, Q. Zhang, L. Zeng, X. Su, C. Xie, and K. Peng, Laser Photon. Rev. **16**, 2200336 (2022)

[14] Y.-S. Ra, A. Dufour, M. Walschaers, C. Jacquard, T. Michel, F. Fabre, and N. Treps, Nat. Phys. **16**, 144 (2020).

[15] K. Takase, J. I. Yoshikawa, W. Asavanant, M. Endo, and A. Furusawa, Phys. Rev. A **103**, 013710 (2021).

[16] W. Asavanant, K. Nakashima, Y. Shiozawa, J. Yoshikawa, and A. Furusawa, Opt. Express **25**, 32227 (2017).

[17] D. V. Sychev, A. E. Ulanov, A. A. Pushkina, M. W. Richards, I. A. Fedorov, and A. I. Lvovsky, Nat. Photon. **11**, 379 (2017).

[18] A. Ourjoumtsev, F. Ferreyrol, R. Tualle-Brouri, and P. Grangier, Nat. Phys. **5**, 189 (2009).

[19] O. Steuernagel and R.-K. Lee, Adding or subtracting a single photon is the same for pure squeezed vacuum states (unpublished).

[20] O. Steuernagel and R.-K. Lee, arXiv:2311.17399.

[21] G. S. Agarwal and K. Tara, Phys. Rev. A **43**, 492 (1991).

[22] C. Quesne, Phys. Lett. A **288**, 241 (2001).

[23] Z. Zhang and H. Fan, Phys. Lett. A **165**, 14 (1992).

[24] A. Zavatta, S. Viciani, and M. Bellini, Science **306**, 660 (2004).

[25] V. Parigi, A. Zavatta, M. Kim, and M. Bellini, Science **317**, 1890 (2007).

[26] A. Zavatta, V. Parigi, and M. Bellini, Phys. Rev. A **75**, 052106 (2007).

[27] M. Dakna, L. Knöll, and D.-G. Welsch, Eur. Phys. J. D **3**, 295 (1998).

[28] M. Dakna, L. Knöll, and D.-G. Welsch, Opt. Commun. **145**, 309 (1998).

[29] C.-M. Wu, S.-R. Wu, Y.-R. Chen, H.-C. Wu, and R.-K. Lee, in *Conference on Lasers and Electro-Optics*, OSA Technical Digest (Optica Publishing Group, San Jose, California United States, 2019).

[30] H.-Y. Hsieh, Y.-R. Chen, J. Ning, H.-C. Wu, H. L. Chen, Z.-H. Shi, P.-H. Wang, O. Steuernagel, C.-M. Wu, and R.-K. Lee, arXiv:2405.02812.

[31] H.-Y. Hsieh, Y.-R. Chen, H.-C. Wu, H. L. Chen, J. Ning, Y.-C. Huang, C.-M. Wu, and R.-K. Lee, Phys. Rev. Lett. **128**, 073604 (2022).

[32] L.-Y. Hu, X.-X. Xu, Z.-S. Wang, and X.-F. Xu, Phys. Rev. A **82**, 043842 (2010).

[33] A. I. Lvovsky, P. Grangier, A. Ourjoumtsev, V. Parigi, M. Sasaki, and R. Tualle-Brouri, arXiv:2006.16985.

[34] G. T. Arman and P. K. Panigrahi, Opt. Lett. **46**, 1177 (2021).

[35] C. Chamberland, K. Noh, P. Arrangoiz-Arriola, E. T. Campbell, C. T. Hann, J. Iverson, H. Putterman, T. C. Bohdanowicz, S. T. Flammia, A. Keller, G. Refael, J. Preskill, L. Jiang, A. H. Safavi-Naeini, O. Painter, and F. G. S. L. Brandão, PRX Quantum **3**, 010329 (2022).

[36] L. Gravina, F. Minganti, and V. Savona, PRX Quantum **4**, 020337 (2023).

[37] D. Gottesman, A. Kitaev, and J. Preskill, Phys. Rev. A **64**, 012310 (2001).

[38] H. M. Vasconcelos, L. Sanz, and S. Glancy, Opt. Lett. **35**, 3261 (2010).

[39] J. E. Bourassa, R. N. Alexander, M. Vasmer, A. Patil, I. Tzitrin, T. Matsuura, D. Su, B. Q. Baragiola, S. Guha, G. Dauphinais, K. K. Sabapathy, N. C. Menicucci, and I. Dhand, Quantum **5**, 392 (2021).

[40] M. Eaton, N. Rajveer, and P. Olivier, New J. Phys. **21**, 113034 (2019).

[41] I. Tzitrin, J. E. Bourassa, N. C. Menicucci, and K. K. Sabapathy, Phys. Rev. A **101**, 032315 (2020).